Title: "Genome-scale methods converge on key mitochondrial genes for the survival of human cardiomyocytes in hypoxia."

Authors: Lindsay M Edwards[a], Martin I Sigurdsson[b,c], Peter A Robbins[d], Michael E Weale[e], Gianpiero L. Cavalleri[f], Hugh E Montgomery[g] and Ines Thiele[h]

Affiliations:

[a] School of Biomedical Science, King's College London, SE1 1UL, UK

[b]Department of Anaesthesia, Perioperative and Pain Medicine, Brigham and Women's Hospital / Harvard Medical School, Boston, USA

[d] Department of Physiology, Anatomy and Genetics, University of Oxford, Oxford, OX1 3PT, UK

[e] Department of Medical and Molecular Genetics, King's College London School of Medicine, London, SE1 9RT, UK

[f] Molecular and Cellular Therapeutics, Royal College of Surgeons in Ireland, 123 St. Stephen's Green, Dublin 2, Ireland

[g] Institute for Human Health and Performance, University College London, N19 5LW, UK

[h] Luxembourg Centre for Systems Biomedicine, University of Luxembourg, Belval, 7, avenue des Hauts-Fourneaux, L-4362 Esch-sur-Alzette, Luxembourg

✉ **Address for Correspondence:**

Dr Lindsay Edwards

Centre of Human & Aerospace Physiological Sciences, King's College London

SH4.15 Guy's Campus

London SE1 1UL.

Tel: +44 (0)20 7848 6978

E-mail: lindsay.edwards@kcl.ac.uk

Running head: Constraint-based modelling, hypoxia and human genetics

Abstract

Background: Any reduction in myocardial oxygen delivery relative to its demands can impair cardiac contractile performance. Understanding the mitochondrial metabolic response to hypoxia is key to understanding ischemia tolerance in the myocardium. We employed a novel combination of two genome-scale methods to study key processes underlying human myocardial hypoxia tolerance. In particular, we hypothesised that computational modelling and evolution would identify similar genes as critical to human myocardial hypoxia tolerance. Methods & Results: We analysed a reconstruction of the cardiac mitochondrial metabolic network using constraint-based methods, under conditions of simulated hypoxia. We used flux balance analysis, random sampling and principle components analysis to explore feasible steady-state solutions. Hypoxia blunted maximal ATP (-17%) and haeme (-75%) synthesis and shrank the feasible solution space. TCA and urea cycle fluxes were also reduced in hypoxia, but phospholipid synthesis was increased. Using mathematical optimization methods, we identified reactions that would be critical to hypoxia tolerance in the human heart. We used data regarding SNP frequency and distribution in the genomes of Tibetans (whose ancestors have resided in persistent high-altitude hypoxia for several millennia). Six reactions were identified by both methods as being critical to mitochondrial ATP production in hypoxia: phosphofructokinase, phosphoglucokinase, Complex II, Complex IV, aconitase and fumarase. Conclusions: Mathematical optimization and evolution converged on similar genes as critical to human myocardial hypoxia tolerance. Our approach is unique and completely novel and demonstrates that genome-scale modelling and genomics can be used in tandem to provide new insights into cardiovascular genetics.

Introduction

Systems biology uses mathematical and computational methods to describe and explore complex biological networks. An important recent trend in systems biology has been the development and application of 'constraint-based modelling' [1]. Constraint-based modelling provides three very significant advantages over traditional mathematical approaches for the study of large and complex biochemical systems. First, very large models (up to thousands of reactions) can be accommodated. Thus the entire metabolic network of a mitochondrion (for example) can be modelled. Second, precise descriptions of the behaviour of each enzyme in the system (i.e. rate laws) are not required. Finally, detailed information regarding the activity of a single protein (for example, whether an enzyme is allosterically modified or not) is not necessary. Thus *unlike traditional 'kinetic' models, constraint-based models do not rely on, nor do they require, detailed knowledge of an enzyme's phosphorylation status (for example), nor the abundance of substrates and products.*

Constraint-based modelling is able to confer these advantages because the underlying models and assumptions are simple. The basic unit for constraint-based modelling is a *network model*, similar to the London Underground map. In the case of a biochemical network, this is constructed using 1) the known presence or absence of reactions based on genomic, proteomic or biochemical data; and 2) the known (species-specific) stoichiometry of all the chemical reactions included in the network. To this basic model are added a series of 'constraints' (from which the method derives its name), including reaction directionality, mass and charge balancing and absolute limits to metabolite uptake and excretion. Unlike traditional enzyme kinetic parameters (e.g. Michaelis-Menten midpoints), many of the underlying assumptions

in constraint-based models are robust to variations in physical environment (such as temperature). However, constraint-based models are not able to simulate the exact behaviour of a biochemical system. Instead, by keeping the underlying assumptions as simple and robust as possible, they attempt to mirror the constraints which the true network faces *in vivo*. Nevertheless, one can predict the most likely behaviour of the system (using Monte Carlo methods) or predict the behaviour of the network at an optimum value of some assumed 'physiological objective'. A more detailed description of the approach can be found in the Methods and Supplemental Materials of the present manuscript, and in many excellent reviews [1-4]. Regarding its utility: constraint-based modelling, using genome-scale metabolic networks, has been used to successfully predict the metabolic signatures of human inherited diseases [5-8], and to permit the *in silico* design of tumour-specific toxins [9] and aid in the design of microbial strains for the purposes of metabolic engineering [10].

Myocardial ischemia and hypoxia, whether cause or consequence, are common features of the failing heart; understanding the mitochondrial response to hypoxia is key to understanding ischemia tolerance. Myocardial hypoxia can be due to any number of factors, but is most commonly caused by coronary artery or microvascular heart disease, exacerbated by increased oxygen demand from ventricular remodelling. Ischaemic heart disease remains the leading cause of death in the developed world; therefore gaining new insights into the mechanisms whereby heart cells can survive hypoxia of any duration is a matter of considerable importance.

Hypoxia, consequent upon a reduction in barometric pressure, is also a consistent environmental challenge for human populations at high altitude, where it has led to a

robustly detectable degree of genetic and phenotypic divergence over evolutionary timescales [11, 12]. Thus human populations at high altitude offer a unique opportunity to study the genetic response to hypoxia. We used a novel combination of genome-scale modelling, mathematical optimization and genome-wide analysis of single nucleotide polymorphisms (SNPs) in humans to study the response of cardiac mitochondria to hypoxia. In particular, we sought to test our hypothesis that if evolution is an optimization process, then mathematical optimization methods, when applied to a metabolic model, would converge on the same set of reactions, critical to environmental (in this case hypoxic) performance. By comparing information from natural (evolution) and mathematical optimization methods we sought to identify key genes and reactions that underlie cardiac tolerance to hypoxia.

Methods

The reconstruction of the human cardiac mitochondrial metabolic network from proteomic and biochemical data was described previously [13]. Briefly, proteomic and transcriptomic data were used to derive an organelle 'metabolic parts list' (i.e. a list of all metabolic proteins known to be associated with a cardiac mitochondrion). These parts were 'connected' by their species-specific stoichiometric chemical equations. The draft reconstruction was extensively tested and manually curated. The final model used herein comprised 195 reactions, 235 metabolites and 25 exchange reactions (for a full description see [13, 14] and the Supplementary Materials). The exchange reactions did not represent genuine biochemical reactions, but instead described the exchanges that were necessary between the network and its environment so that a steady-state could be achieved. Having reconstructed the network, a series of limits or 'constraints' were added, all of which constrained the upper and lower limits of metabolite exchange of the model with its environment (e.g. oxygen, glucose). These constraints are in Supplementary Table 1 and represent maximum and minimum flux rates in human heart mitochondria *in vivo*. To simulate hypoxia, we reduced the upper constraint on oxygen uptake in the model to 25% of baseline values (normoxia), from 39.1 $\mu M\ min^{-1}$ (g mitochondrial protein)$^{-1}$ (henceforth shortened to U) to 9.775 U. Our choice of simulating severe hypoxia was motivated by an intention to highlight any effects; however, it is worth noting that complete anoxia can occur in regions of ischemic myocardium (e.g. during acute myocardial infarction).

Computational analysis of network models rarely leads to a single set of predicted fluxes. Instead, methods are used to analyze the possible combinations of fluxes that allow a steady-state, given the applied constraints. The solutions together are termed

the feasible steady-state solution space. Alternatively, one can use linear optimization to compute a set of fluxes that optimize the value of a given objective function, an approach typically referred to as flux balance analysis (FBA). For example, this method would return a set of fluxes that correspond to the highest possible rate of ATP production by the network, if ATP production was the objective function. When conducting FBA, we optimized the mitochondrial network for three objective functions (phospholipid, haeme and ATP synthesis) [13]. Alternate optimal solutions (i.e. other sets of fluxes that also gave an optimal objective) were accounted for via flux variability analysis (see below). We also studied the optimization of all three objectives simultaneously (see Supplementary Materials for details). This method comprises placing the objective functions under study into hierarchical order (for example, haeme biosynthesis then phospholipid biosynthesis then ATP synthesis). The network is optimized for the first objective, then optimized for the second with the first held at optimal value and so forth.

We used two computational methods to identify reactions that are critical to hypoxia tolerance in the mitochondria metabolic network – shadow prices [15] and flux spans [16]. Shadow prices have been used in metabolic network analysis before [15, 17]. Shadow prices (also known as Lagrange multipliers) are measures of the degree to which the value of the objective function is affected by the availability of a particular resource. For example, if ATP synthesis were the objective function, a shadow price of 1.0 for glucose (for example) would indicate that a 1 unit increase in glucose availability would lead to an equivalent increase in ATP synthesis. A shadow price of 2.0 would indicate that a unit increase in the availability of glucose would result in a two unit increase in ATP synthesis, and so forth. We reasoned therefore that reactions for

168 which metabolites with large, positive shadow prices were either substrates or
169 products, would be crucial to hypoxic performance (at least, for the objective function
170 under investigation). To assess the likelihood that our method had outperformed
171 chance, we used simple permutation testing.
172
173 Our second approach was to use flux spans. Using flux variability analysis [18] we
174 computed the range of values that flux through each reaction could take at an
175 optimum (computed using FBA). Taken together, these ranges delineate the set of
176 alternate optimal solutions (i.e. different sets of fluxes that result in the same optimal
177 value of the objective) [18]. By calculating the difference between the upper and lower
178 feasible fluxes we derived a flux span for each reaction. Here we express these as a
179 relative ratio. Hence a reaction with flux = 10 U and with the lower and upper feasible
180 fluxes being 8 and 12 U respectively would have a relative flux span of 0.4 (or 40%).
181 We reasoned that reactions with the smallest relative flux spans would be critical to
182 hypoxia tolerance and hypoxic performance. Again, we used permutations to estimate
183 the probability that our method had outperformed chance alone.
184
185 We used data from a genome-wide allelic differentiation scan (GWADS) comparing
186 SNP frequencies of Tibetans (n = 35) residing at 3200-5000 m, with 84 individuals
187 from the founder population. Subjects were recruited from three distinct regions of
188 China: the North Western region of Yunnan province, Mag Xiang and Zhaxizong
189 Xiang (both in the Tibet Autonomous Region). Genotypic data from the HapMap
190 Phase III Han population were also included. These data have been analyzed
191 previously[11] and full details can be found in this earlier publication. Each gene was
192 assigned a genome-wide p-value that serves as an estimate of the degree of selective

pressure applied to that gene (through differences in SNP frequency). Details regarding the calculation of these *p*-values can also be found elsewhere [11]. We extracted the *p*-values corresponding to the genes in our model and ranked genes by smallest GWADS *p*-value first, producing a list of nuclear-encoded mitochondrial genes with an accompanying measure of selective pressure in humans living in persistent hypoxia.

Where appropriate, means and standard deviations are given. However, modelling results are often a single datum point (e.g. differences in optimal ATP synthesis rate, determined using flux balance analysis, under hypoxia and normoxia) and are therefore given as such.

Results

We optimized the network for three physiological 'targets' (objective functions) - ATP, haeme and phospholipid biosynthesis [13] – using flux balance analysis (FBA) [1]. Hypoxia reduced the optimal ATP synthesis rate by 13%, from 45.8 to 36.6 U. Figure 1 shows a quantized heatmap of the accompanying differences in flux. There were reductions in flux through many reactions comprising the TCA cycle and oxidative phosphorylation. There were also reductions in flux through most reactions comprising fatty acid uptake, transport, activation and oxidation, although some were maintained due to the imposition of a minimum uptake rate (this is a physiological constraint imposed by the ability of fatty acids to diffuse freely across membranes). Glycolytic rates were similar, which was expected as maximal ATP synthesis was the objective. The flux through multiple reactions required for phospholipid biosynthesis were increased and the demand reaction was activated in hypoxia. To ensure that the degree of simulated hypoxia affected our results quantitatively but not qualitatively, we performed additional flux balance analysis experiments at various intermediate oxygen uptake rates. The results are in Supplementary Figure 1. Briefly, maximal ATP synthesis was progressively reduced by increasing hypoxia. Consistent with our interpretation, phospholipid biosynthesis was not activated until O_2 uptake dropped below a critical level, at which point a 'sink' for fatty acid carbons was required. There was no evidence of qualitative shifts in carbon flux as maximal O_2 uptake rate was progressively reduced.

Haeme synthesis was blunted by 75% in hypoxia (hypoxia: 0.650 vs. normoxia: 2.44 U). The pattern of flux differences between the optimized network in normoxia and hypoxia was similar to that with ATP synthesis as the objective. Flux through

reactions comprising the TCA cycle, oxidative phosphorylation, the urea cycle and haeme synthesis itself were suppressed. There were increases in long-chain (C20:4 and C22:6) activation and an increase in phospholipid biosynthesis. A heatmap of differences in flux across the network under these conditions (haeme biosynthesis as the objective function in hypoxia vs. normoxia) is given in Supplementary Figure 2. However, when phospholipid biosynthesis was the objective it was unchanged by oxygen restriction, at 22.8 U.

We then performed multiple objective analyses with three different hierarchies of objective functions. 1. ATP > haeme > phospholipid: In normoxia, and with ATP synthesis fixed at its optimal value of 45.8 U, haeme and phospholipid synthesis were eliminated. In hypoxia, with ATP synthesis fixed at its optimal value of 36.6 U, haeme synthesis was still eliminated; however, optimized phospholipid biosynthesis was now non-zero, although reduced ~100-fold at 0.265 U. 2. Haeme > phospholipid > ATP: In normoxia, with haeme biosynthesis at its optimal rate of 2.44 U, both phospholipid and ATP synthesis were abolished. In hypoxia, with haeme biosynthesis at 0.650, phospholipid biosynthesis was possible and optimized to 0.867 U; ATP synthesis was abolished. 3. Phospholipid > haeme > ATP: As maximal phospholipid biosynthesis was unaffected by hypoxia it was fixed at 0.867 U for both conditions (normoxia/hypoxia). In both normoxia and hypoxia, haeme biosynthesis gained optimal values the same as those where it was the only objective function considered (normoxia: 2.44 U vs. hypoxia: 0.650 U). In normoxia, ATP biosynthesis was subsequently limited to 8.85 U; in hypoxia it was reduced far less, to 19.3 U. A summary of all the optima is in Supplementary Table 2.

We next used uniform random sampling [19], a method that characterizes the steady-state solution space without requiring an objective function. Figure 1b shows a quantized heatmap of differences in median flux. Consistent with the FBA results, fluxes through reactions comprising oxidative phosphorylation, the TCA cycle and fatty acid metabolism were reduced in hypoxia. Without the requirement to maximize ATP synthesis in normoxia that was elsewhere imposed by FBA, glycolytic flux increased in hypoxia. The heatmap shows a reduction in flux through lactate dehydrogenase and the lactate transporter; however, this represents a *reversal* in flux, from uptake to efflux. Also noteworthy is a reduction in urea cycle flux in hypoxia.

We analysed the sampled data using principal components analysis (PCA), allowing us to visualize patterns of change. We modelled the sampled data together and found that five components captured 65% of the total variance. When plotted, the scores on these components revealed that hypoxia substantially reduced the dimensions of the solution space, reducing the flexibility of the metabolic network even though the dimensions of the space were the same. This was especially apparent in principal components 1 and 2 (Figure 2), with principal component 1 being dominated by reactions related to gas exchange, the TCA cycle and oxidative phosphorylation and principal component 2 being dominated by reactions related to iron transport and haeme biosynthesis.

Given that optimal phospholipid biosynthesis was unaffected by oxygen restriction, we continued by studying those metabolites and reactions that limited optimal ATP and haeme biosynthesis in the mitochondrial metabolic network under hypoxia. We first computed shadow prices for all metabolites in the model when optimising the

network for either ATP or haeme synthesis. Table 2 gives metabolites with the largest positive shadow prices and the corresponding twenty discrete reactions for each objective function. Three classes of metabolite (and reaction) dominated: long-chain (>20C) fatty acid transport, glycolysis and haeme biosynthesis. When optimising for ATP synthesis, the largest shadow prices were several-fold larger than when optimising for haeme synthesis (e.g. 4.0 for cytosolic fructose diphosphate, fdp(c), vs. 1.2 for cytosolic arachidonic acid, c206(c)). When optimizing the network with ATP synthesis as the objective function, the metabolites with large positive shadow prices were mainly related to glycolysis, oxidative phosphorylation and the TCA cycle.

We next computed flux spans, using flux variability analysis. The reactions with the smallest relative flux spans when optimizing the network for either haeme or ATP synthesis are given in Table 3. As with shadow prices, the magnitude of the parameter (in this case, relative flux span) was several fold different when optimizing ATP vs. haeme synthesis; in both cases the difference (larger shadow prices and smaller flux spans) was consistent with ATP synthesis being more tightly restricted by hypoxia. Interestingly, reactions related to oxidative phosphorylation both had narrow flux spans regardless of whether ATP or haeme synthesis were the objectives. In particular, complex IV of the respiratory chain was ranked in the top two (Table 3). Perhaps unsurprisingly, reactions related to proto-haeme synthesis and iron transport also had small relative flux spans when optimizing for haeme synthesis. When optimizing the network for ATP synthesis, reactions from the TCA cycle and glycolysis were highly represented.

We generated a complete list of nuclear-encoded mitochondrial genes with a

corresponding measure of selective pressure at high altitude. The twenty 'most selected' genes (i.e. smallest *p*-value) are in Table 1. Using permutations, we assessed the likelihood that mathematical optimization had outperformed chance when predicting genes under pressure. When conducting shadow price analysis with ATP synthesis as the objective, we selected the 16 metabolites with the largest positive shadow price corresponding to 20 discrete reactions shown in Table 2. Of these 20 reactions, two (phosphofructokinase (PFK) and phosphoglycerate kinase (PGK)) carried flux and corresponded to genes in Table 1. However, permutation testing suggested that random selections of 16 metabolites would equal or outperform our modelling approach most of the time ($p = \sim 0.860$). We observed that two of the only three metabolites with shadow prices of 3 or greater when optimizing the network for either objective (cytosolic fructose 6-phosphate and fructose diphosphate, f6p(c) and fdp(c) respectively in Table 2) are both substrate and product for PFK, the most 'heavily selected' gene in Table 1. We next compared the reactions highlighted by shadow price analysis whilst optimizing the network for haeme synthesis. Three reactions were common with those in Table 1: hydroxymethylbilane synthase (HMBS), porphobilinogen synthase (PPBNGS) and phosphoglycerate kinase (PGK). Once again, permutations suggested that shadow pricing had not outperformed chance when identifying genes under pressure.

We used a similar approach to assess the performance of flux span analysis. Table 3 shows that flux span analysis identified three (haeme synthesis) and six (ATP synthesis) reactions that were common with those that were the most heavily selected genes in Table 1. With ATP synthesis as the objective, we used permutation testing to assess whether modelling had outperformed chance when predicting genes under

pressure. Random selections only matched flux span analysis 1675 out of 100000 times, offering evidence that this approach had outperformed chance at $p < .05$.

We repeated this process with haeme synthesis as the objective function. Using 100000 permutations, random selection matched the model performance approximately half the time ($p = \sim 0.525$). Hence using flux span analysis with haeme as the objective had not outperformed chance.

Discussion

Myocardial hypoxia can be either acute or chronic and occurs whenever oxygen delivery is insufficient to meet the needs of the contracting myocardium. This can be due to any combination of reduced O_2-carrying capacity due to anaemia, reduced haemoglobin saturation (whether environmental or pathological), poor cardiac output or compromised blood flow due to coronary artery or microvascular heart disease, and increased oxygen demand associated with stress or structural remodelling (e.g. ventricular hypertrophy). Ischaemic heart disease remains the leading cause of death in the developed world. A notable feature of heart failure is that, once left ventricular dysfunction has been established, patients suffer a relentless apoptotic loss of viable cardiomyocytes that some investigators believe to be due to repeated, transient ischaemic and hypoxic events [20]. Therefore understanding the mechanisms whereby heart cells can survive either transient or sustained hypoxia and ischaemia is a matter of considerable importance. Here we present an entirely new approach to this question using systems biology methods that encompass genomics, metabolic modelling and mathematical optimization.

We first studied the effect that hypoxia had on the solution space (the set of all feasible fluxes) of the reconstructed cardiac mitochondrial metabolic network using two complementary methods – optimization (FBA) and Monte Carlo sampling. Optimization requires an objective function; in keeping with previous work we studied three objectives that are central to mitochondrial function: the synthesis of ATP, haeme and mixed phospholipids [13]. Although maximal phospholipid synthesis was unaffected by hypoxia, both haeme and ATP synthesis were reduced (by 75% and 13% respectively). The reduction in maximal ATP synthesis was accompanied by

reductions in TCA cycle flux, oxidative phosphorylation and fatty acid uptake and processing but a seemingly paradoxical increase in phospholipid biosynthesis.

The degree to which maximal haeme synthesis was blunted in hypoxia was striking. This 75% loss of proto-haeme synthesis capacity was accompanied by many of the metabolic features observed when optimizing ATP production in hypoxia. Haeme is a major component of haemoglobin, itself substantially increased in response to hypoxia to enhance systemic oxygen transport [21]. Thus network stoichiometry forms a constraint to haeme biosynthesis that may partly define the speed with which haeme can be synthesized in hypoxia. Non iron-deficient anaemia is a common feature in heart failure patients, yet its aetiology is unknown [22]. Furthermore, many studies have shown that reduced haemoglobin is an independent predictor of risk in heart failure patients [23, 24], although again the mechanism remains poorly understood. Our simulations suggest that hypoxia itself can cause significant reductions in proto-haeme synthesis, both in the heart and elsewhere, and that hypoxia of any kind could lead to a vicious cycle of blunted haeme synthesis, reduced O_2-carrying capacity in blood and subsequently worsened hypoxaemia. Furthermore, in cultured human neurons, haeme deficiency causes a decrease in (haeme-containing) complex IV (cytochorome c oxidase) and activation of nitric oxide synthase [25]. Given that complex IV release is a key component of the p53 apoptotic cascade [26], this suggests an intriguing new avenue for investigations into hypoxia-induced myocyte apoptosis.

We studied the effect on mitochondria of forcing them to balance competing objectives in hypoxia. When ATP production was given hierarchical 'superiority' (as is almost certainly the case *in vivo*), haeme synthesis was completely abolished in

normoxia and hypoxia. Thus haeme and ATP synthesis compete for the same resources; quite moderate reductions in O_2 supply, coupled with increases in ATP demand, might lead to profound reductions in haeme synthesis capacity due to stoichiometric constraints in the metabolic network. Interestingly, phospholipid biosynthesis was abolished in normoxia under this hierarchy but was active in hypoxia. This was likely due to competition with ATP synthesis for lipids; in hypoxia, ATP synthesis was diminished freeing up lipids for phospholipid synthesis.

We next studied the set of feasible solutions using random sampling. Multiple random samples of the solution space allow the generation of probability density functions for flux through every reaction; the most probable value can often predict the measured *in vivo* rate [14]. As with linear optimization (FBA) we observed reductions in TCA cycle and oxidative phosphorylation reactions, in addition to a reduction in urea cycle flux. This last is intriguing because flux through arginosuccinate synthetase (*ASS*) was decreased in simulated hypoxia. *ASS* been elsewhere been reported as a target of the von Hippel-Lindau tumour suppressor gene (*VHL*) [27], an inverse regulator of HIF-1α. Manipulation of *VHL* expression led to corresponding changes in ASS levels in RCC10 renal cell carcinoma cells.

Once again we observed that many of the reactions required for phospholipid biosynthesis were increased and the biosynthesis reaction itself was activated in hypoxia. Without this redirection of fatty acid flux, the imposition of hypoxia, combined with minimum uptake rates for fatty acids, would have led to an accumulation of unoxidized fatty acids in the model and a loss of homeostasis. Cardiac mitochondria face an identical challenge *in vivo* and redirect fatty acids to

storage (away from oxidation) when ischaemic [28]. Similarly, Langendorff-perfused hearts exposed to acute hypoxia increase phospholipid biosynthesis to maintain lipid homeostasis [29]. We also observed an increase in glycolytic flux (Figure 1B).

Overall, the pattern of change in metabolic flux in our simulations was strikingly consistent with experimental observations of cellular responses to hypoxia, including the reduction in flux through pyruvate dehydrogenase (PDHm) *in vivo* that is brought about by modulation of pyruvate dehydrogenase kinase [30]. It is interesting to note that the reduction in flux through PDHm in our simulations directly resulted from network stoichiometry, without any additional explanation or control. While the notion that glycolytic flux is increased in hypoxia is certainly not new, altered (particularly increased) lipid biosynthesis in response to hypoxia is a less often considered component of hypoxia tolerance. Previous investigators have reported both increased [29, 31] and decreased [32] lipid synthesis in hypoxia in model systems. These discrepancies may be due to differences in isotope labelling strategy (e.g. acetate vs. glycerol vs. palmitate) or outcome measure. However, there is no question that lipids accumulate in the heart in response to hypoxia and ischaemia [28]. It should be noted that the details of whole heart lipid-handling in hypoxia and/or ischemia may be different to the mitochondrial response considered in isolation. It is interesting also that lipotoxicity – defined as a chronic mismatch between oversupply of acetyl-CoA from lipid breakdown and its subsequent mitochondrial oxidation – is a stoichiometric disorder and can be as readily caused by impaired oxidative phosphorylation (for example, by hypoxia) as lipid oversupply. The consistency of our simulations with experimental observations reinforced to us the notion that our methods were both robust and relevant.

We sought to test whether mathematical optimization had converged on the same reactions that human evolution had identified as being critical to optimal hypoxic function. We used data from a GWADS scan comparing SNP frequencies of Tibetans residing at 3500 m (and whose ancestors have 'lived high' for over 10,000 years [33]) with individuals from the HapMap Phase III Chinese Han sample, who are closely related but have resided at sea level throughout [11]. Tibetans were ideal for this study because, despite systemic adjustments (for example, increased breathing rates), they continue to have lower arterial oxygen content than sea-level dwellers [34].

It is interesting that the largest shadow prices were recorded when optimizing the mitochondrial metabolic network for ATP synthesis in hypoxia. This suggests that, even in the case of competing objectives, increasing the supply of these metabolites would be especially advantageous when oxygen supply is limited (either by environment or pathology). The metabolite with the largest shadow price in any analysis we conducted was fructose diphosphate, a product of phosphofructokinase (PFK). However, permutation testing failed to support the notion that shadow prices and evolution had converged on similar reactions.

The results gained by examining flux spans were more compelling. Flux spans are the range of values within which a reaction rate can lie at a computed optimum. We reasoned that reactions with narrow flux spans would be under greater selective pressure. We generated a list of reactions with the smallest flux spans (yet which carried flux) and compared these with the SNP data. When we optimized for ATP synthesis, the results supported the notion that mathematical optimization and

463 evolution had converged on similar reactions (where 6/20 reactions were common
464 between the two selections). The common reactions selected by flux span analysis and
465 evolution were related to haeme synthesis (although only when optimizing for haeme
466 synthesis), glycolysis (PFK, PGK), the TCA cycle (aconitase and fumarase) and
467 oxidative phosphorylation (Complexes II and IV). We propose that our combined
468 method has identified reactions that are especially important in maintaining or
469 increasing mitochondrial ATP synthesis in the hypoxic heart. This view is supported
470 by the existing literature. For example, it was recently reported that mice exposed to
471 three weeks of normobaric hypoxia had reduced Complex II, IV and aconitase activity
472 in cardiac mitochondria [35] while fumarate accumulation leads to 'pseudo-hypoxic'
473 activation of HIF-1α [36], suggesting that many of the same reactions highlighted here
474 indeed have important roles in hypoxic adaptation and, hence, survival. Our combined
475 approach also yielded an unexpected benefit: Computational analysis was able to
476 provide suggestions as to whether genes were under positive or negative selective
477 pressure (an important distinction to which traditional genome-wide analytical
478 techniques are blind).
479
480 A final note regarding PFK: basic biochemistry textbooks all highlight the importance
481 of PFK as a key regulatory step in glycolysis (e.g. page 444 in [37]). Yet there is a
482 tautology here: PFK is heavily regulated biologically (for example, by ATP/AMP,
483 fructose 2,6-bisphosphate [37] etc.). However its heavy regulation is evidence for, not an
484 explanation of, its importance. We note that in our simulations, using multiple
485 objectives and alternative analytical strategies, PFK was repeatedly highlighted as
486 being an important determinant of the objective. Our model contained no information
487 whatsoever regarding biological regulation (for example, allosteric modulation by

other small molecules). In other words, our simulations suggest that PFK is important because it occupies a critical point in the metabolic network due to network topology and nothing more. By extension, this protein is likely to be under strong evolutionary selective pressure in many environments, leading to complex phenotypic properties. Once again this was supported in the genetic data, at least in hypoxia.

Limitations

Our main hypothesis - that evolution and mathematical optimization would converge on similar targets – was supported. In so doing we generated a list of genes that the two methods independently highlighted as potentially important for hypoxic survival. Although we believe that the nature of our combined approach adds additional support to the significance of these genes, we wish to stress that genes identified by any genome-wide method should be treated as 'candidates' only. Direct experimental evidence will always be required to clarify the function of each. Of course, for some of the genes identified by our approach, overwhelming evidence already exists confirming their importance (for example, pyruvate dehydrogenase [30, 38, 39]).

A second limitation relates to possible differences in the Han vs. Tibetan environment beyond simply altitude (e.g. diet and temperature). Several points are pertinent:

1. Although temperatures may differ between the two locations, most very high altitude populations descend lower in winter;

2. Diet may differ; however many essential elements (reliance on vegetables and use of rice) are similar;

3. Multiple studies have utilized the Han vs Tibetan genome comparison. All have found the same primary hit (EPAS1), which is a gene regulating expression of a hypoxia-responsive transcription factor;

4. The candidates in the present study were chosen because computational analysis of a separate network model suggested their role in hypoxia. This makes it more likely that this was indeed the cause and is, potentially, another benefit of our approach.

Disclosure

HM was, from 2011-13, contracted as a consultant to GSK relating to development of a drug in the field of hypoxia. However, no involvement was needed and he received no payment. IT was supported in part by an ATTRACT programme grant (FNR/A12/01) from the Luxembourg National Research Fund (FNR).

References

1. Lewis NE, Nagarajan H, Palsson BO. Constraining the metabolic genotype-phenotype relationship using a phylogeny of in silico methods. *Nat Rev Microbiol*. 2012;10:291-305
2. Bordbar A, Palsson BO. Using the reconstructed genome-scale human metabolic network to study physiology and pathology. *J Intern Med*. 2012;271:131-141
3. Oberhardt MA, Palsson BO, Papin JA. Applications of genome-scale metabolic reconstructions. *Mol Syst Biol*. 2009;5:320
4. Edwards LM, Thiele I. Applying systems biology methods to the study of human physiology in extreme environments. *Extreme Phys Med*. 2013;2
5. Sigurdsson MI, Jamshidi N, Jonsson JJ, Palsson BO. Genome-scale network analysis of imprinted human metabolic genes. *Epigenetics*. 2009;4:43-46
6. Smith AC, Robinson AJ. A metabolic model of the mitochondrion and its use in modelling diseases of the tricarboxylic acid cycle. *BMC Syst Biol*. 2011;5:102
7. Shlomi T, Cabili MN, Ruppin E. Predicting metabolic biomarkers of human inborn errors of metabolism. *Mol Syst Biol*. 2009;5:263
8. Thiele I, Swainston N, Fleming RMT, Hoppe A, Sahoo S, Aurich MK, Haraldsdottir H, Mo ML, Rolfsson O, Stobbe MD, Thorleifsson SG, Agren R, Bolling C, Bordel S, Chavali AK, Dobson P, Dunn WB, Endler L, Hala D, Hucka M, Hull D, Jameson D, Jamshidi N, Jonsson JJ, Juty N, Keating S, Nookaew I, Le Novere N, Malys N, Mazein A, Papin JA, Price ND, Selkov E, Sigurdsson MI, Simeonidis E, Sonnenschein N, Smallbone K, Sorokin A, van Beek JHGM, Weichart D, Goryanin I, Nielsen J, Westerhoff HV, Kell DB,

549 Mendes P, Palsson BO. A community-driven global reconstruction of human
550 metabolism. *Nat Biotech*. 2013;advance online publication
551 9. Frezza C, Zheng L, Folger O, Rajagopalan KN, MacKenzie ED, Jerby L,
552 Micaroni M, Chaneton B, Adam J, Hedley A, Kalna G, Tomlinson IP, Pollard
553 PJ, Watson DG, Deberardinis RJ, Shlomi T, Ruppin E, Gottlieb E. Haem
554 oxygenase is synthetically lethal with the tumour suppressor fumarate
555 hydratase. *Nature*. 2011;477:225-228
556 10. Hua Q, Joyce AR, Fong SS, Palsson BO. Metabolic analysis of adaptive
557 evolution for in silico-designed lactate-producing strains. *Biotechnol Bioeng*.
558 2006;95:992-1002
559 11. Beall CM, Cavalleri GL, Deng L, Elston RC, Gao Y, Knight J, Li C, Li JC,
560 Liang Y, McCormack M, Montgomery HE, Pan H, Robbins PA, Shianna KV,
561 Tam SC, Tsering N, Veeramah KR, Wang W, Wangdui P, Weale ME, Xu Y,
562 Xu Z, Yang L, Zaman MJ, Zeng C, Zhang L, Zhang X, Zhaxi P, Zheng YT.
563 Natural selection on epas1 (hif2alpha) associated with low hemoglobin
564 concentration in tibetan highlanders. *Proc Natl Acad Sci U S A*.
565 2010;107:11459-11464
566 12. Yi X, Liang Y, Huerta-Sanchez E, Jin X, Cuo ZX, Pool JE, Xu X, Jiang H,
567 Vinckenbosch N, Korneliussen TS, Zheng H, Liu T, He W, Li K, Luo R, Nie
568 X, Wu H, Zhao M, Cao H, Zou J, Shan Y, Li S, Yang Q, Asan, Ni P, Tian G,
569 Xu J, Liu X, Jiang T, Wu R, Zhou G, Tang M, Qin J, Wang T, Feng S, Li G,
570 Huasang, Luosang J, Wang W, Chen F, Wang Y, Zheng X, Li Z, Bianba Z,
571 Yang G, Wang X, Tang S, Gao G, Chen Y, Luo Z, Gusang L, Cao Z, Zhang Q,
572 Ouyang W, Ren X, Liang H, Huang Y, Li J, Bolund L, Kristiansen K, Li Y,

573 Zhang Y, Zhang X, Li R, Yang H, Nielsen R, Wang J. Sequencing of 50
574 human exomes reveals adaptation to high altitude. *Science*. 2010;329:75-78
575 13. Vo TD, Greenberg HJ, Palsson BO. Reconstruction and functional
576 characterization of the human mitochondrial metabolic network based on
577 proteomic and biochemical data. *J Biol Chem*. 2004;279:39532-39540
578 14. Thiele I, Price ND, Vo TD, Palsson BO. Candidate metabolic network states
579 in human mitochondria. Impact of diabetes, ischemia, and diet. *J Biol Chem*.
580 2005;280:11683-11695
581 15. Savinell JM, Palsson BO. Network analysis of intermediary metabolism using
582 linear optimization. I. Development of mathematical formalism. *J Theor Biol*.
583 1992;154:421-454
584 16. Ghosh A, Zhao H, Price ND. Genome-scale consequences of cofactor
585 balancing in engineered pentose utilization pathways in *saccharomyces*
586 *cerevisiae*. *PLoS ONE*. 2011;6:e27316
587 17. Varma A, Boesch BW, Palsson BO. Stoichiometric interpretation of
588 escherichia coli glucose catabolism under various oxygenation rates. *Appl*
589 *Environ Microbiol*. 1993;59:2465-2473
590 18. Mahadevan R, Schilling CH. The effects of alternate optimal solutions in
591 constraint-based genome-scale metabolic models. *Metabolic engineering*.
592 2003;5:264-276
593 19. Kaufman DE, Smith RL. Direction choice for accelerated convergence in hit-
594 and-run sampling. *Operations Research*. 1998;46:84-95
595 20. Sabbah HN, Sharov VG, Goldstein S. Cell death, tissue hypoxia and the
596 progression of heart failure. *Heart Fail Rev*. 2000;5:131-138

21. Martin D, Windsor J. From mountain to bedside: Understanding the clinical relevance of human acclimatisation to high-altitude hypoxia. *Postgrad Med J*. 2008;84:622-627; quiz 626
22. Coats AJ. Anaemia and heart failure. *Heart*. 2004;90:977-979
23. Sharma R, Francis DP, Pitt B, Poole-Wilson PA, Coats AJS, Anker SD. Haemoglobin predicts survival in patients with chronic heart failure: A substudy of the elite ii trial. *European Heart Journal*. 2004;25:1021-1028
24. Go AS, Yang J, Ackerson LM, Lepper K, Robbins S, Massie BM, Shlipak MG. Hemoglobin level, chronic kidney disease, and the risks of death and hospitalization in adults with chronic heart failure: The anemia in chronic heart failure: Outcomes and resource utilization (anchor) study. *Circulation*. 2006;113:2713-2723
25. Atamna H, Killilea DW, Killilea AN, Ames BN. Heme deficiency may be a factor in the mitochondrial and neuronal decay of aging. *Proc Natl Acad Sci U S A*. 2002;99:14807-14812
26. Schuler M, Bossy-Wetzel E, Goldstein JC, Fitzgerald P, Green DR. P53 induces apoptosis by caspase activation through mitochondrial cytochrome c release. *Journal of Biological Chemistry*. 2000;275:7337-7342
27. Harten SK, Esteban MA, Maxwell PH. Identification of novel vhl regulated genes by transcriptomic analysis of rcc10 renal carcinoma cells. *Adv Enzyme Regul*. 2009;49:43-52
28. Scheuer J, Brachfeld N. Myocardial uptake and fractional distribution of palmitate-1 c14 by the ischemic dog heart. *Metabolism*. 1966;15:945-954

29. Chabowski A, Gorski J, Calles-Escandon J, Tandon NN, Bonen A. Hypoxia-induced fatty acid transporter translocation increases fatty acid transport and contributes to lipid accumulation in the heart. *FEBS Lett*. 2006;580:3617-3623
30. Kim JW, Tchernyshyov I, Semenza GL, Dang CV. Hif-1-mediated expression of pyruvate dehydrogenase kinase: A metabolic switch required for cellular adaptation to hypoxia. *Cell Metab*. 2006;3:177-185
31. Harris P, Gloster J. The effects of acute hypoxia on lipid synthesis in the rat heart. *Cardiology*. 1971;56:43-47
32. Cheng P, Hatch GM. Inhibition of cardiolipin biosynthesis in the hypoxic rat heart. *Lipids*. 1995;30:513-519
33. Aldenderfer M. Moving up in the world: Archaeologists seek to understand how and when people came to occupy the andean and tibetan plateaus. *Am Sci*. 2003;91:542-529
34. Beall CM. Two routes to functional adaptation: Tibetan and andean high-altitude natives. *Proc Natl Acad Sci U S A*. 2007;104 Suppl 1:8655-8660
35. Heather LC, Cole MA, Tan JJ, Ambrose LJ, Pope S, Abd-Jamil AH, Carter EE, Dodd MS, Yeoh KK, Schofield CJ, Clarke K. Metabolic adaptation to chronic hypoxia in cardiac mitochondria. *Basic Res Cardiol*. 2012;107:268
36. Ashrafian H, O'Flaherty L, Adam J, Steeples V, Chung YL, East P, Vanharanta S, Lehtonen H, Nye E, Hatipoglu E, Miranda M, Howarth K, Shukla D, Troy H, Griffiths J, Spencer-Dene B, Yusuf M, Volpi E, Maxwell PH, Stamp G, Poulsom R, Pugh CW, Costa B, Bardella C, Di Renzo MF, Kotlikoff MI, Launonen V, Aaltonen L, El-Bahrawy M, Tomlinson I, Pollard PJ. Expression profiling in progressive stages of fumarate-hydratase

deficiency: The contribution of metabolic changes to tumorigenesis. *Cancer Res*. 2010;70:9153-9165

37. Berg JM, Tymoczko JL, Stryer L. Glycolysis. *Biochemistry*. 2002.

38. Mora A, Davies AM, Bertrand L, Sharif I, Budas GR, Jovanovic S, Mouton V, Kahn CR, Lucocq JM, Gray GA, Jovanovic A, Alessi DR. Deficiency of pdk1 in cardiac muscle results in heart failure and increased sensitivity to hypoxia. *EMBO J*. 2003;22:4666-4676

39. Papandreou I, Cairns RA, Fontana L, Lim AL, Denko NC. Hif-1 mediates adaptation to hypoxia by actively downregulating mitochondrial oxygen consumption. *Cell Metab*. 2006;3:187-197

Table 1: Nuclear genes encoding mitochondrial proteins: the twenty 'most selected' (i.e. smallest GWADS *p*-values) in Tibetan high-altitude natives

Entrez ID	Gene name	GWADS min P	Reaction
5230	'PGK1'	0.000427922	'PGK'
5211	'PFKL'	0.000562071	'PFK'
4696	'NDUFA3'	0.001056733	'NADH2-u10m'
34	'ACADM'	0.002100322	All 'FAOX'
435	'ASL'	0.003329005	'ARGSL'
539	'ATP5O'	0.003329005	'ATPS4m'
27068	'PPA2'	0.004127063	'PPAm'
2937	'GSS'	0.004425362	'GTHS'
8170	'SLC14A2'	0.004892165	'UREAt'
4715	'NDUFB9'	0.005012697	'NADH2-u10m'
7991	'TUSC3'	0.005679664	'NADH2-u10m'
3145	'HMBS'	0.006801907	'HMBS'
10476	'ATP5H'	0.008432045	'ATPS4m'
4709	'NDUFB3'	0.00856278	'NADH2-u10m'
50	'ACO2'	0.008803353	'ACONTm'
2271	'FH'	0.008830507	'FUMm'
1350	'COX7C'	0.01011429	'CompIVr1'
4697	'NDUFA4'	0.01011429	'NADH2-u10m'
210	'ALAD'	0.010792961	'PPBNGS'
23761	'PISD'	0.011201573	'PSDm'

Table 2: Metabolites with the largest positive shadow prices when optimising the mitochondrial metabolic network for either haeme or ATP synthesis (and corresponding reactions)

Optimize haeme synthesis			**Optimize ATP synthesis**		
Metabolite	*Shadow price*	*Reaction(s)*	*Metabolite*	*Shadow price*	*Reaction(s)*
c204(c)	1.30	C204 (1)§, C204t (1)	fdp(c)	4	**PFK*** (1), FBA (2)
c204coa(c)	1.30	C204, C204CRN1 (1), C204CRN3 (1)	f6p(c)	3	**PFK***, PGI (3)
c204crn(c)	1.30	C204CRN1, C204CRN2 (1)	g6p(c)	3	HEX1 (4), PGI, G6PI#
c204coa(m)	1.30	C204CRN3, **FAOXC204*#**	13dpg(c)	2.20	**PGK*** (5), GAPD (6)
c204crn(m)	1.30	C204CRN2, C204CRN3	c204coa(c)	2	C204 (7), C204CRN1 (8), C204CRN3 (9)
pheme(m)	1.00	FCLTm (6)	c204crn(c)	2.00	C204CRN1, C204CRN2 (10)
ppp9(m)	1.00	PPPGOm (6), FCLTm,	dhap(c)	2.00	TPI (11), FBA, G3PDm (12)
pppg9(c)	0.86	CPPPGO (8), PPPG9tm (8)	g3p(c)	2.00	FBA, G3PATm (13), G3PDm, GAPD, TPI
pppg9(m)	0.86	PPPG9tm, PPPGOm,	glc-D(c)	2.00	GLCt1 (14), HEX1
cpppg3(c)	0.76	CPPPGO, UPPDC1 (9)	c204coa(m)	2.00	C204CRN3, **FAOX204*#**
hmbil(c)	0.76	**HMBS* (10)**, UPP3S (11)	c204crn(m)	2.00	C204CRN2, C204CRN3
uppg3(c)	0.76	UPP3S, UPPDC1	2pg(c)	1.19	ENO, PGM,
ppbng(c)	0.19	**HMBS***, **PPBNGS* (12)**	3pg(c)	1.19	**PGK***, PGM
5aop(c)	0.10	**PPBNGS***, 5AOPtm (13)	pep(c)	1.19	PYK, CITtbm
5aop(m)	0.10	5AOPtm, ALASm (14)	succoa(m)	0.81	AKGDm, ALASm#, OCOAT1m#
succoa(m)	0.10	AKGDm (15), ALASm, OCOAT1m#	akg(c)	0.62	ICDHxm (20), ICDHym#, TYRTAm#, AKGDm
13dpg(c)	0.05	**PGK*** (16), GAPD (17)			

2pg(c)'	0.0476 19048	ENO, PGM,			
13dpg(c)	0.0476 19048	**PGK***, GAPD			

§Bracketed numbers are reaction rank based on metabolite shadow price
#Flux through this reaction was zero
*Corresponding gene is one of the 'twenty most selected' in Table 1

Table 3: Reactions with the smallest relative flux spans when optimising the mitochondrial metabolic network for either **a:** haeme synthesis or **b:** ATP synthesis

a. Optimize haeme synthesis[#]			**b. Optimize ATP synthesis**		
Reaction	Relative flux span ($\times 10^{-6}$)	Rank	Reaction	Relative flux span ($\times 10^{-6}$)	Rank
CompIVr1*	1.2	1	ATPtm	0.01	1
CYOR-u10m	1.2	1	**CompIVr1***	0.10	2
NADH2-u10m*	1.3	3	CYOR-u10m	0.10	3
CPPPGO	1.4	3	SUCOASm	0.20	4
FCLTm	1.4	3	ENO	0.21	5
FE2t1	1.4	3	GAPD	0.21	6
FE2tm	1.4	3	**PGK***	0.21	7
HMBS*	1.4	3	PGM	0.21	8
PPPG9tm	1.4	3	FBA	0.21	9
UPP3S	1.4	3	GLCt1	0.21	10
UPPDC1	1.4	3	HEX1	0.21	11
PPPGOm	1.4	3	**PFK***	0.21	12
5AOPtm	1.4	3	PGI	0.21	13
AKGDm	1.4	3	TPI	0.21	14
ALASm	1.4	3	**ACONTm***	0.22	15
ASPGLUm	1.4	3	AKGDm	0.22	16
ASPTAm	1.4	3	CSm	0.22	17
GLYt2r	1.4	3	ICDHxm	0.22	18
GLYtm	1.4	3	**NADH2-u10m***	0.27	19
MDHm	1.4	3	**FUMm***	0.29	20
PPBNGS*	1.4	3			

[#]21 reactions due to 'drawn ranking'
*Corresponding gene is one of the 'twenty most selected' in Table 1

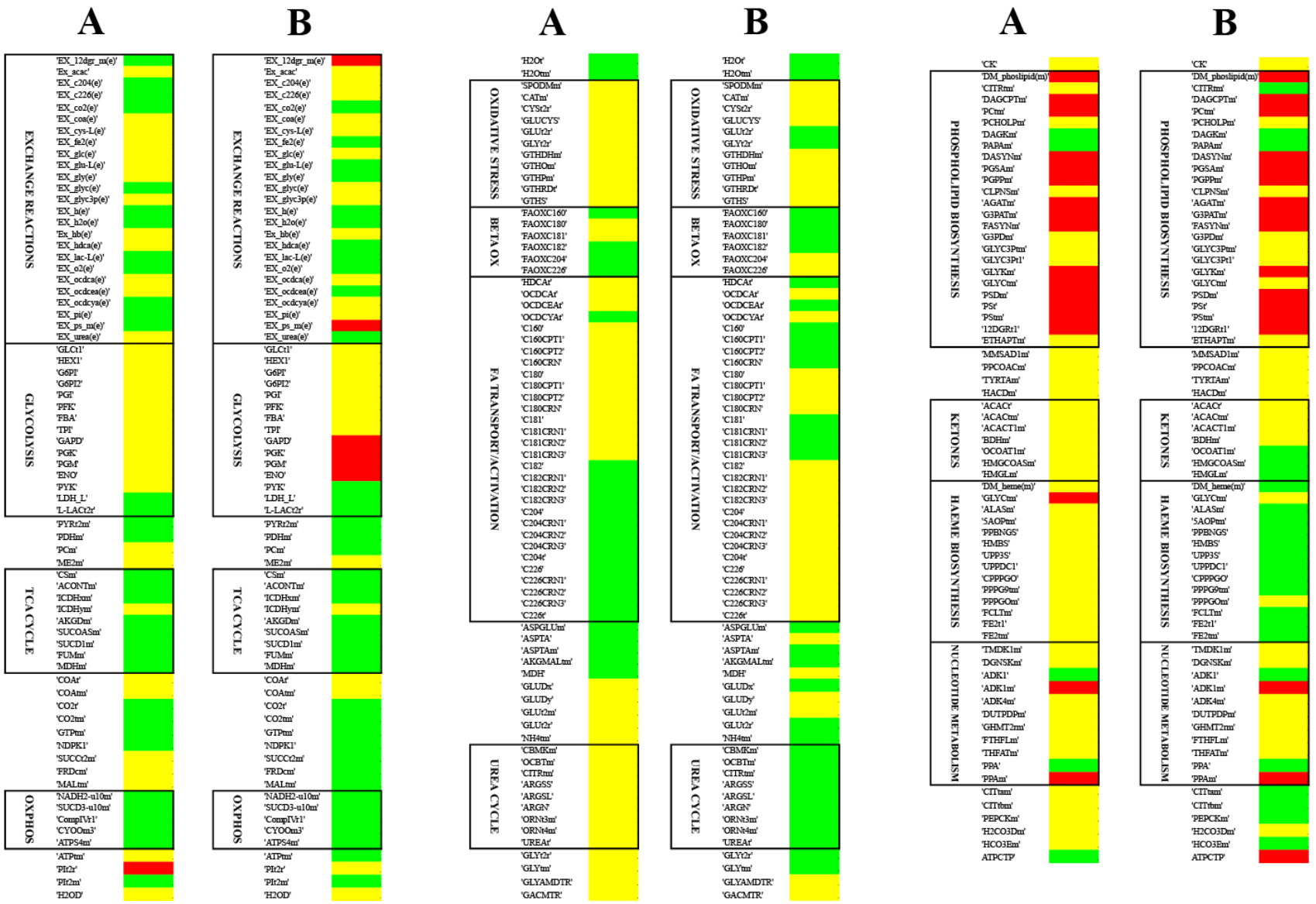
A
B
A
B
A
B
EXCHANGE REACTIONS
GLYCOLYSIS
TCA CYCLE
OXPHOS
OXIDATIVE STRESS
BETA OX
FA TRANSPORT/ACTIVATION
UREA CYCLE
PHOSPHOLIPID BIOSYNTHESIS
KETONES
HAEME BIOSYNTHESIS
NUCLEOTIDE METABOLISM

Figure 1: Heatmap showing the effect of hypoxia on flux distribution in the mitochondrial metabolic network. Red = flux increased by > 0.1 U; green = flux decreased by > 0.1 U; yellow = flux changed by < 0.1 U..**A:** Flux balance analysis, with ATP synthesis as the objective function. **B:** Uniform random sampling. (U = $\mu m\ min^{-1}\ g^{-1}$)

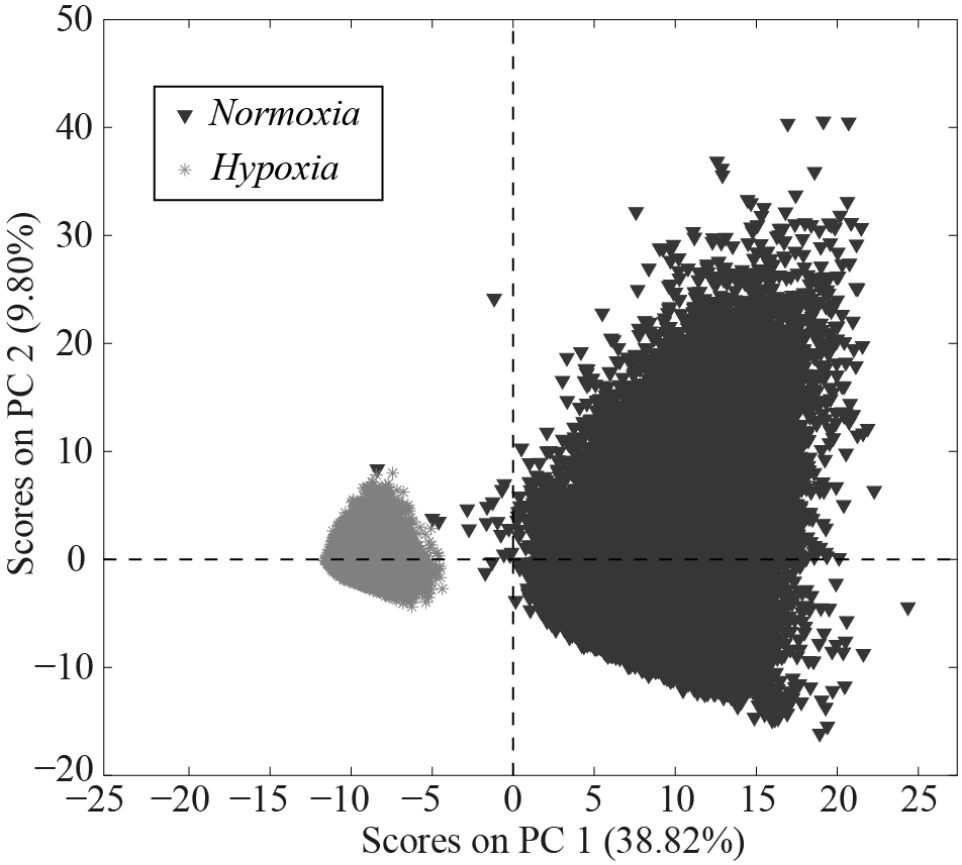

Figure 2: Biplot showing scores on principal component 1 vs. scores on principal component 2. Both components are from a five-component PCA model of data sampled in hypoxia and normoxia. Black triangles = normoxia; grey stars = hypoxia.